

Trajectories entropy in dynamical graphs with memory

Francesco Caravelli^{1,2,3}

¹*Invenia Labs, 27 Parkside Place, Parkside, Cambridge CB1 1HQ, UK and*

²*London Institute of Mathematical Sciences, 35a South Street, London W1K 2XF, UK*

³*Department of Computer Science, University College London, Gower Street, London WC1E 6BT, UK*

In this paper we investigate the application of a non-local graph entropy to evolving and dynamical graphs. The measure is based upon the notion of Markov diffusion on a graph, and relies on the entropy applied to trajectories originating at a specific node. In particular, we study the model of reinforcement-decay graph dynamics, which leads to scale free graphs. We find that the node entropy characterizes the structure of the network in the two parameter phase-space describing the dynamical evolution of the weighted graph. We then apply an adapted version of the entropy measure to purely memristive circuits. We provide evidence that meanwhile in the case of DC voltage the entropy based on the forward probability is enough to characterize the graph properties, in the case of AC voltage generators, one needs to consider both forward and backward based transition probabilities. We provide also evidence that the entropy emphasizes the self-organizing properties of memristive network, which re-organizes itself to satisfy the symmetries of the underlying graph.¹

I. INTRODUCTION

The theory of complex networks has found applications in many fields across the natural sciences. Until recently, most of the studies performed in complex networks concerned static graphs. Preferential attachment [1] is the most well known mechanism for constructing scale-free networks, and it concerns in fact a specific type of growth of graphs in order to explain the properties of realistic, well known networks (rich gets richer phenomenon). Scale free networks are defined by the distribution $P(k)$ of the degrees of connectivity, which obeys a power law $P(k \gg 1) \approx k^{-\rho}$, with k being the number of connections of a given node. The exponent ρ is typically in the range between 2 and 3 ; moreover, many realistic networks turn out being also small-world [1–6].

Several models in which preferential attachment is an emergent property have been proposed in the physics literature [7–13], and inspired by the networks of memristors, we proposed a model of dynamical graphs in which two competing mechanisms take place: a graph "evaporation" (or decay), and a reinforcement process due to the diffusion of particles on the graph. Recently, the interest has shifted towards the understanding of dynamical phenomena of graphs. In this article, we present new results on a class of dynamical models that gives rise to scale-free graphs by means of what we call *memory*. Memory is an ubiquitous and necessary requirement to give rise to complex phenomena in plenty of contexts. In this model, memory is represented by non-markovianity, as the reinforcement process changes the particles hopping probabilities.

The main result obtained in [14] is that the interplay between random growth of the graph, decay of the links

and their strengthening performed by random walkers hoping over them, leads to the generation of scale free graphs. Thus, although the model is local (in the sense of evolution rules which are local on the graph), it is from the temporal point of view a non-local one. Interestingly, real condensed-matter systems shows some degree of memory in their response functions (e.g., its resistance) when subject to external perturbations [15]. A similar memory mechanism is used as an optimization procedure by ants in order to find the shortest path, by reinforcing with pheromones the most walked paths [16, 17], and has been shown to be employed by networks of memristors (resistors with memory) [18, 19] to solve optimization problems such as the maze [20] or other shortest-path problems [21]. Recently, it has been argued that several "hard" problems can be solved in polynomial time using memristors [22].

In the case of dynamical graphs it is hard (if not impossible) to characterize with a few numbers the general and topological properties of the dynamics, in particular if the rules of evolution are non-local, as for instance in the case of memristors. In the present paper we provide evidence that for the specific case of two dynamical graph models, such as the reinforcement-decay and memristive graph model evolutions, the evolution properties can be characterized by a non-local graph entropy. Following this line of thought, we tentatively study the properties of the resulting graph using a measure of graph entropy introduced in [23]. This measure of graph complexity is based on the idea that for the case of graphs, in order to give a non-local characterization of a node based on the macroscopic connectivity properties, one needs to consider higher order loops in the graph. This method is inspired by the macroscopic notions of entropy introduced in [24, 25] and applied to the Markov chain transition probabilities of the weighted graph which change dynamically. If M denotes the Markov transition matrix, one

¹Part of this work was presented at the 7th workshop on Guided Self-Organization, Freiburg, Germany (2014) and at the Symposium on Complexity, Computation and Criticality in Sydney (2015).

can define the (local) entropy of a state i as:

$$S(i) = - \sum_j M_{ij} \log(M_{ij}), \quad (1)$$

with M_{ij} being the Markov operator. M can be derived from a graph \mathcal{G} , given a positive adjacency matrix A , by normalizing over rows or columns. However, eqn. (1) is completely local and does not consider the fact that, in order to account for longer walks on the graph, entropy necessitates an extension to account non-local (global) effects. Similar ideas were also considered in Ekroot and Cover to introduce the entropy of Markov trajectories in [26], and in the complex networks community. In the present paper we consider the extension considered in [23], which relies on the definition of Markov probabilities not on the local diffusion probability of a node, but on the probability of trajectories *originated* at a specific node.

The paper is organized as follows. In Section II A we provide the algorithm for the toy model of reinforcement-decay introduced in a previous work, and give further arguments for its robustness. In Section II B we introduce the HP memristors and their behavior. In Section II C we recall the graph entropy measure considered in this work to analyze the properties of dynamical graphs. We then apply the graph entropy in Sections III A and III B for the reinforcement-decay model and memristive networks respectively. Conclusions follow.

II. MATERIAL & METHODS

A. Reinforcement-decay dynamical graphs

In this section we recall the model introduced in [14]. This model was introduced to study a simplified dynamics mimicking systems of ants (reinforcing walkers) and as a toy model for studying graphs with memory.

Model. — The algorithm to dynamically modify the graph is based upon the following steps:

a) Initialization: We start with a weighted random graph of N_0 nodes. The weights are drawn with constant probability in $[0, 1]$, and $P \leq N_0$ particles are randomly placed.

After initialization, a cycle of the algorithm consists of the steps of Hopping, Strengthening/Decay, and Growth:

b) Hopping: We let the particles hop between nodes i and j with probability p_{ij} proportional to the link strength $p_{ij} = A_{ij}/\sum_j A_{ij}$, where A_{ij} is the weighted adjacency matrix of the graph.

c) Strengthening/Decay: All the links hopped on by the particles in the last L steps are reinforced by γ . Links with strength less than threshold L_d decrease their strength by α , with probability p_d , and are removed when they reach a negative weight.

A critical ingredient to obtain scale free graphs was shown to be:

d) Growth: At this step, a new node is added (and with probability p_p a new particle is placed on it). The new node connects to each of the previously existing nodes with probability p_{nl} , here chosen to be one, and with random weights with constant probability in $[0, 1]$.

The memory feature of this model lays in the non-markovianity of the particles hopping. Each time a particle hops through an existing link, this is reinforced, and thus the probability of hopping on it increases. We note that the decay process competes with the reinforcing one. The interplay between these two phenomena has been shown to lead to a critical growth of the effective graph, obtaining in fact asymptotic degree distributions which are scale free. The observation that the growth in the graph is a crucial step for scale free degree distribution is made by imposing the growth to stop at a certain maximum number of nodes N_c . After the growth stops, one observes that graph properties change abruptly and the scale free degree distribution is lost. The model considered here is a form of rich-gets-richer mechanism, and has been inspired by travelling ants leaving an evaporating track of pheromones, and by memristors, which have similar properties. As described in the Appendix of [14], the observation of the scale free degree distribution law can be made precise in the statistical sense and derived analytically. Here we provide the background, giving further arguments of why the algorithm is robust. The equation for the evolution of the degree can be extended to include fluctuations. In fact one has an effective evolution of the degree k_s of the node s with time:

$$k_s(t+1) = k_s(t) - \alpha k_s(t) + p_s \sum_{i=1}^N w_{si}, \quad (2)$$

where w_{si} are independent random variables drawn from a constant probability distribution $P(x) = 1$. We note that when $N \gg 1$, due to the central limit theorem, we have that $\sum_{i=1}^N w_{si} \approx \mathcal{N}(\frac{N}{2}, \frac{\sqrt{N}}{\sqrt{12}})$, where $1/12$ is the variance of the distribution, and $\frac{N}{2}$ is its mean. This implies that in the large N limit, we can describe the evolution of the degree of the graph as a stochastic differential equation of the form:

$$dk_s(t) = \left(p_s \frac{N}{2} - \alpha k_s(t) \right) dt + p_s \tilde{\sigma} dW_t, \quad (3)$$

where dW_t is an *effective* Wiener differential, and where we defined $\tilde{\sigma} = \frac{\sqrt{N}}{\sqrt{12}}$. Since p_s is an independent variable, we can trace out this degree of freedom in the differential equation (3) by taking the mean. Using standard formulae for the mean and the variance, we can thus write the compact effective equation:

$$\begin{aligned} \langle dk_s(t) \rangle_{p_s} &= \left(\frac{1}{2} - \alpha k_s(t) \right) dt + \frac{1}{N} \tilde{\sigma} dW_t \\ &= \left(\frac{1}{2} - \alpha k_s(t) \right) dt + \frac{1}{\sqrt{12N}} dW_t \end{aligned} \quad (4)$$

The stochastic differential equation of eqn. (4) of the same form as obtained in [14], but with the addition of a stochastic term. Here we extend it to including the stochastic term. We note that eqn. (4) is a stochastic differential equation of the form:

$$dk = (ak + c)dt + (bk + d)dW_t, \quad (5)$$

for the function $k(t)$, where the constants are given by

$$a = -\alpha \quad (6)$$

$$b = 0 \quad (7)$$

$$c = \frac{1}{2} \quad (8)$$

$$d = \frac{1}{\sqrt{12N}}. \quad (9)$$

If we define the function Φ_t given by,

$$\Phi_t(t, W_t) \equiv \exp((a - b^2/2)t + bW_t) = \exp(-\alpha t), \quad (10)$$

the solution of the differential equation of eqn. (4) is given by [27]:

$$\begin{aligned} k_s(t) &= \Phi_t \left(k_s^0 + \frac{1}{2} \int_0^t \Phi_s^{-1} ds + \frac{1}{\sqrt{12N}} \int_0^t \Phi_s^{-1} dW_s \right) \\ &= e^{-\alpha t} \left(k_s^0 + \frac{1}{2} \int_0^t e^{\alpha s} ds + \frac{1}{\sqrt{12N}} \int_0^t e^{\alpha s} dW_s \right) \\ &= e^{-\alpha t} \left(k_s^0 + \frac{1}{2} \frac{e^{\alpha t} - 1}{\alpha} + \frac{1}{\sqrt{12N}} \int_0^t e^{\alpha s} dW_s \right) \end{aligned} \quad (11)$$

where k_s^0 represents the initial condition. Using the fact that $\langle \int_0^t I(s) dW_s \rangle_{W_t} = 0$ for all smooth and deterministic processes $I(s)$, we obtain the solution as a function of t :

$$\langle k_s(t) \rangle_{W_t} = e^{-\alpha t} \left(k_s^0 + \frac{1}{2} \frac{e^{\alpha t} - 1}{\alpha} \right). \quad (12)$$

The constant k_s^0 can be related to the node s using the boundary conditions at a certain initial time t_0 . It is easy to evaluate the variance of this process at time t , being given by the stochastic term. Using the Itô isometry formula, we note that $\text{Var}[k_s(t)] = \frac{1}{12N} \int_0^t e^{2\alpha s} ds = \frac{1}{12N} \frac{(e^{2\alpha t} - 1)}{2\alpha}$. This solution is the same as the one obtained in [14], which was confirmed by means of numerical simulations, and exhibiting very robust scale free distributions under parameter perturbations. We note however that since the variance of the process scales as $1/N$, this implies that the larger the graph, the smaller the deviation from the asymptotic distribution. This might explain the robustness of the scale-free property observed numerically.

B. Memristive networks

A memristor can be thought simply as a resistance which depends on an internal state which changes dynamically in time. Memristors are in fact passive components which perform analog computation: computing in

memory is in fact one of the newly formed paradigms in which novel non-Turing computational scenarios involve memory elements which store and process information in the same physical location [28]. Although this new form of computation could, in principle, be performed using CMOS technology, the most promising and energy-effective implementation relies upon the use of memristive, memcapacitive and meminductive units [29]. These components could find a plethora of applications in electronics for building bio-inspired circuitry aimed at performing neuromorphic computation.

One of the interesting features of memristors is that these can be used both in analog or digital mode, and in combination with CMOS components [15]. Several applications have been found for memristors, such as their use in memcapacitive neural networks, and the possibility of performing logical operations directly within memory using memelements. This latter feature is of particular interest to solve the long-standing von Neumann bottleneck problem of modern computers and solve NP-hard problems in polynomial *time* [22]. Being these passive component, the use of memelement for low energy dissipating circuits is a further appealing feature.

Being memristive component involved in the solution of optimization problems, it is important to know how fast circuits made of memristor relax to an asymptotic equilibrium configuration of the memristences. This implies that studying the emergence of the solution of an optimization problem can be thought as a relaxation phenomenon, which is typical of statistical physics problems in condensed matter. In this paper we will thus try to infer global, non-local properties of memristive networks using insights which arouse in the context of network theory. A memristive component can be described by the following set of equations

$$V(t) = R(w, t)I(t), \quad (13)$$

$$\dot{w} = f(w, I), \quad (14)$$

where $I(t)$ is the current in the memristor at time t , $V(t)$ is the applied voltage, R is memristance which depends on the state of the system and can vary in time, w is a set of n state variables describing the internal state of the system, and f is a continuous n -dimensional vector function.

For the present paper we consider the case of a linear memristor of HP-type [18], which can be described by the equations:

$$V(t) = R(w, t)I(t) \quad (15)$$

$$\dot{w} = p \frac{\mu R_{on}}{2d} I = \frac{p}{\beta} R_{on} I \quad (16)$$

$$\begin{aligned} R(w, t) &= R_{on}(1 - w(t)) + R_{off}w(t) \\ &= R_{on}[1 + (r - 1)w(t)], \end{aligned} \quad (17)$$

where $p = \pm 1$ and represents the polarity of the memristor, R_{on} is the limiting resistance when the memristor is in the conducting phase, R_{off} is the resistance in the insulating

phase ; we defined $r = \frac{R_{off}}{R_{on}}$, usually assumed to satisfy the relation $r \gg 1$.

This is the simplest model proposed in the literature, but more realistic ones include state decay. In fact, [30–32] realistic physical models include also an extra term proportional to the weight. The internal parameter dynamics equation can be thus extended to include an exponential decay term of the form:

$$\dot{w} = \frac{p}{\beta} R_{on} I - \alpha w. \quad (18)$$

where α represents the decay parameter. Assuming for instance that I is constant asymptotically, dynamically one obtains a fixed point in the internal memory parameter, $w(\infty) \propto I$, which can be different from the boundary values $w = 0, 1$.

A network of pure memristors satisfies the laws of standard, linear circuit theory. Given in fact a generic network of resistances, the currents satisfy the constraints given by:

$$\vec{v} = \hat{R}(w(t)) \vec{i} + \vec{s} \quad (19)$$

$$\hat{G} \vec{i} = 0 \quad (20)$$

where the first equation represents simply the relation between the voltage on each branch k of the network v_k , the current in that branch i_k , the eventual voltage sources s_k and each resistance. The matrix \hat{G} simply implements the conservation of currents at each node, which can be thought as a constraint. For the case of memristors, the matrix \hat{R} , and each diagonal element contains the resistance of each memristor at time t , $R_{kk}(t) \equiv R_k(w_k(t))$. If the memristors are of the HP type, then one has to introduce also an equation for the internal memory parameters $\dot{w}_k(t) = f(w_k, I_k)$, and impose that constraints on their domain, e.g. $0 \leq w_k(t) \leq 1$.

In this paper we study a specific network configuration, which enjoys several symmetries. We consider in fact the network considered in Fig. 1, made of L layers. Each layer k contains 2^k memristors connected in triangles, representing a tree. The node at the top of the graph is connected to one side of the voltage generator, and those at the bottom are connected to the other one, and all connected to the ground in order to respect the graph symmetries. We consider this specific graph due to its many symmetries (i.e. intuitively we expect that nodes on each layer should have the same properties and current configurations for instance) and for the sake of simplicity in implementing the dynamics and constructing the graph. We will moreover consider the situation in which the initial internal parameters are chosen at random with constant probability.

In this paper we analyze the structure of memristor networks using a non-local trajectory entropy, and associated with each node.¹

C. Graph entropy

Here we recall the network complexity measure introduced in [23]. The goal is to obtain a graph entropy, based on the Markov transition probability on a graph, which is able to characterize nodes individually.

Given a graph represented by a positive adjacency matrix A , the Markov forward (backward) transition probabilities can be derived using $M_{ij} = \frac{A_{ij}}{\sum_j A_{ij}}$ ($M_{ij} = \frac{A_{ij}}{\sum_j A_{ji}}$). As we will see shortly, the entropy is based upon the notion of probability applied to a particular trajectory in the set of states of a Markovian discrete dynamics and originating at a particular state. Given a the Markovian transition probabilities between two states (nodes of the graph), it is possible to derive the probability of certain trajectories γ , here denoted as $\tilde{M}(\gamma)$. We denote $\{\gamma_i^k\}$ the set of trajectories of length k and originating at i . For instance, if the path is given by $\gamma = \{i, j, k\}$, the probability of that trajectory will be given by $M(\gamma) = M_{ij} M_{jk}$. It is easy to show that $(\{\gamma_i^k\}, \tilde{M}(\{\gamma_i^k\}))$ is a probability space, and thus $M(\gamma_i)$ can be interpreted as probabilities, as $\sum_{\{\gamma_i^k\}} \tilde{M}(\gamma_i^k) = \sum_{j_1, j_2, \dots, j_k} \tilde{M}(\{i, j_1, \dots, j_k\}) = 1$. Also, all elements are clearly positive if the adjacency matrix has only non-negative elements and there are no isolated nodes. We observe that $\tilde{M}(\gamma_i^k)$ is a node-dependent quantity, is non-local, and can be interpreted as a probability measure over the space of walk of fixed length originated at a node. We observe that one could write for instance the normalized entropy

$$({}^{k+1}\vec{S})_i = -\frac{1}{k} \sum_{\{\gamma_i^k\}} \tilde{M}(\gamma) \log(\tilde{M}(\gamma)), \quad (21)$$

but due to the Cesàro mean rule, converges in the limit $k \rightarrow \infty$ to the same value independently from the initial node i . Although this quantity being important, it does not provide a measure which differentiates the nodes. An alternative normalization has thus to be considered.

As shown in [23], interesting properties arise if one chooses a different and multiplicative normalization, on the set of trajectories of length k , defined as:

$${}^{k+1}\vec{S}_\epsilon = -\epsilon^{k-1} \sum_{\{\gamma_i^k\}} \tilde{M}(\gamma) \log(\tilde{M}(\gamma)), \quad (22)$$

where $M(\gamma)$ is the probability associated with the trajectory γ . The parameter ϵ can be chosen arbitrarily, but in order to guarantee convergence in the limit $k \rightarrow \infty$ it has to satisfy $\epsilon < 1$. We note that evaluating the entropy from eqn. (22) computationally hard as it involves the evaluation of an exponential number of trajectories with the length k . Thankfully, such entropy satisfies a recursion relation in terms of the Markov transition matrix M ,

¹ The author is happy to disclose the code made to generate these

simulations upon request.

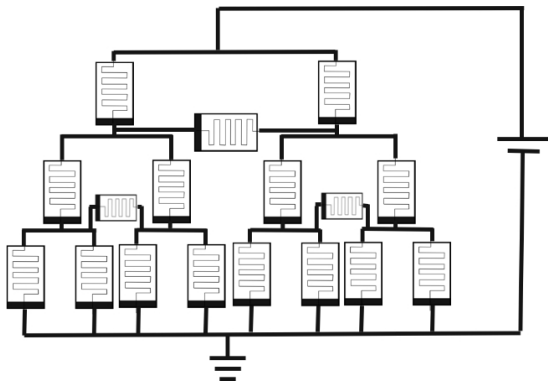


FIG. 1: Memristive circuit defined recursive as on a tree and made of L layers. The nodes in the bottom layer are connected to the ground.

${}^1\vec{S}$ and the parameter $\epsilon < 1$:

$${}^{k+1}\vec{S}_\epsilon = \epsilon^k \left(\frac{M}{\epsilon^{k-1}} \quad {}^k\vec{S} + \quad {}^1\vec{S} \right). \quad (23)$$

If we write down all the terms, recursively, we find:

$${}^{k+1}\vec{S}_\epsilon = \sum_{n=0}^k \epsilon^n M^n \quad {}^1\vec{S}, \quad (24)$$

and, realizing that we can take the limit $k \rightarrow \infty$ safely, we obtain a closed expression :

$${}^*\vec{S}_\epsilon = \frac{1}{I - \epsilon M} \quad {}^1\vec{S}, \quad (25)$$

which is finite for all values of $\epsilon < 1$, is a fixed point of eqn. (23), and can be interpreted as a non-local notion of entropy. We note that now each node has different values of the entropy depending on the Markov transition matrix M . The strength of eqn. (25) is that now it is easier to evaluate than eqn. (22). This advantage comes however at the price of a free parameter ϵ , that can be given an *a posteriori* interpretation if we consider this as a probability over the length of the trajectories. Given this interpretation, the average length of a trajectory becomes:

$$\langle k \rangle = \sum_{k=1}^{\infty} \epsilon^k k = \frac{\epsilon}{(1 - \epsilon)^2}, \quad (26)$$

which can be inverted for any $\langle k \rangle > 0$, for $\epsilon(\langle k \rangle)$. In this paper we consider ϵ such that $\langle k \rangle = N$, the total number of nodes of the networks. In general, the limit $\epsilon \rightarrow 0$ recovers the node entropy considered in other works, as for instance in [21], of which ours can be considered as a non-local extension, and which has been shown to characterize the local behavior of currents. We will consider this extended notion of graph entropy to characterize the dynamics of memristive networks.

It is worth discussing explicitly few properties of the entropy above. We observe first that the limit $\lim_{\epsilon \rightarrow 1} {}^*\vec{S}_\epsilon$

is unbounded. This is due to the fact that the Perron root of a Markov chain is 1 and that thus the resolvent of the operator does not exist. However, eqn. (22) for finite k is indeed bounded from above by $\epsilon^{k-1} k \log(N)$, which is the extreme value of the entropy for finite k , corresponding to a complete graph with N nodes. We note that this entropy goes to infinity in the limit $k \rightarrow \infty$ if and only if $\epsilon \geq 1$. If we set $\langle k \rangle = N$, we can obtain an approximate upper bound for the fixed point entropy of every node by inverting for $\epsilon(N)$ in eqn. (26), and given by:

$${}^*S \lesssim 2^{1-N} N \left(\frac{2N + \sqrt{4N + 1} + 1}{N} \right)^{N-1} \log(N) \quad (27)$$

which is, for $N \gg 1$, of the order of $S \approx N \log(N)$, which unsurprisingly is not an extensive quantity with respect to the addition of new nodes. As a general feature of entropic measures, observing a decrease in graph entropy implies that some structure is being generated dynamically, rather than converging towards a random configuration. As a last comment, we note that this definition does not lead to a unique definition of transition probability when the network is directed. In this case, one can define the *forward* probability, as the one used above, or the *backward* probability. For a directed adjacency matrix, one has the in-degree and the out-degree, defined as diagonal matrices:

$$D_{ii}^{in} = \sum_j A_{ij}, \quad (28)$$

$$D_{ii}^{out} = \sum_j A_{ji}, \quad (29)$$

and thus one has two definitions of transition probabilities:

$$M^f = (D^{out})^{-1} A, \quad (30)$$

$$M^b = (D^{in})^{-1} A^T. \quad (31)$$

Both these definitions will be used in the following.

The entropy introduced in this section shifts compresses the information about the graph into the nodes. Thus, it has the advantage to be *non-local*, with support on the nodes of the graph, and to include all the possible trajectories in the graph.

III. RESULTS

In this section we discuss the results obtained after simulating both models of dynamical graphs with memory introduced previously.

A. Toy diffusion model

In this section we analyze the topological properties of the evolving network under the reinforcement-decay model using the graph entropy of Section II C.

We simulate the system for various values of the two main parameters: the particles creation probability p_p versus the decay probability p_d . We show the values of the entropy as a function of time in Fig. 2. These were obtained averaging over 30 simulations, for fixed parameters $\gamma = 0.1$, $L_d = 1$. At each time step, the strength of links are decreased with probability p_d of a value which we fix to $\alpha = 0.1$. The graph grows at each time step up to a maximum number of nodes N_c , here chosen to be 500, and then the links which have not been established “evaporate”. The stop of the growth is introduced artificially to observe the change and importance of growth for the overall graph configuration. The new link parameter p_{nl} is fixed to 0.1 in the simulations. For each new node, a new particle is injected into the graph with probability p_p . In Fig. 2 we show the evolution of the graph entropy for varying p_d and p_p .

As a first comment, we note that as the graph grows

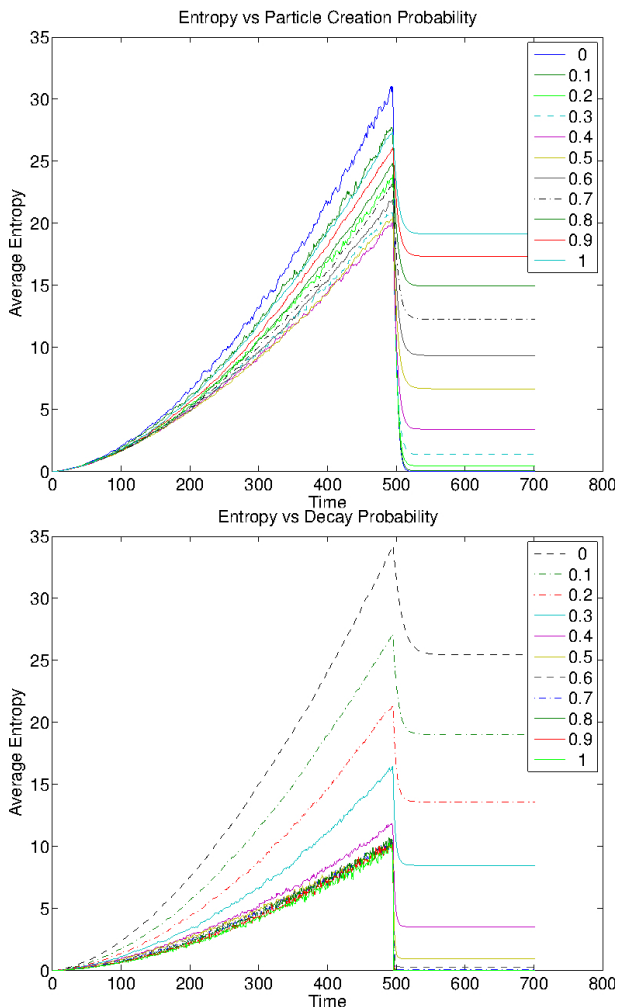


FIG. 2: Evaluation of the mean entropy as a function of time in the reinforcement-decay model. The growth of the graph stops at $T = 500$, and afterwards the network converges, for the case of variation of the particle creation probability (top) and the decay probability (bottom).

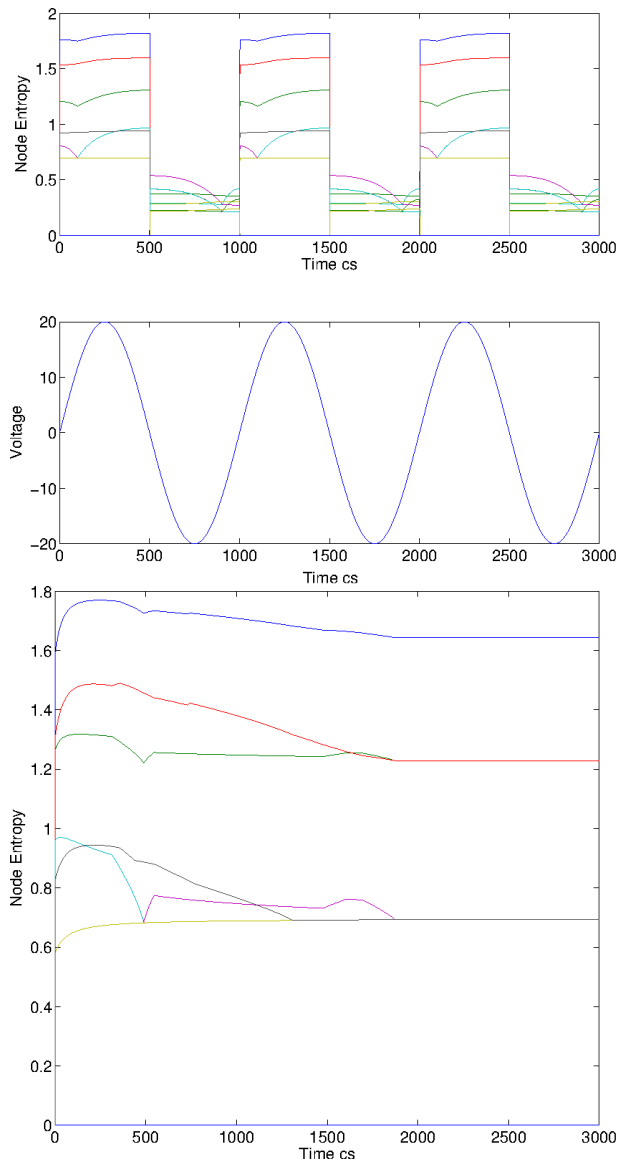


FIG. 3: Evolution of the node entropy for AC and DC voltage, measured in centiseconds for random initial conditions for $L = 4$. *Top*: Evolution of the entropy for the tree graph of Fig. 1 when an AC voltage is applied to the network with $V = 10 \sin(10t)$ volts. *Bottom*: Entropy evolution for the tree graph of Fig. 1 for a DC voltage $V = 60$ volts.

the mean graph entropy, defined as $\langle S \rangle = \frac{1}{N} \sum_{i=1}^N ({}^* S_\epsilon)_i$ (i.e. the average over the nodes), grows as well. Although the mean of the entropy does not have a thermodynamical interpretation, this gives a succinct graphical representation of the outcome. The growth is in general due to both the decrease in the number of nodes to the lack of structure due to the random growth, and to the effect of decay, which tends to destroy the effect of particles creating order and thus less randomness. We note that after the growth stops, the entropy decreases to a stable value. This implies that the effect of decay is of creating

”structure”. This is due to the fact that the graph reduces to the stable link only.

We observe that there is an entropy curve for each set of parameters, both during the growth and after. This implies that this graph entropy measure is enough to characterize the asymptotic state of the graph in the simulations we have performed. We note that the non-local graph entropy is changing both in the case of the decay probability, as in Fig. 2 (top) and for the case of varying particle creation probability, as in Fig. 2 (bottom). In all the simulations, the average entropy per node is indeed characterizing the parameter space.

B. Purely Memristive networks

In the previous section we noted that the graph entropy introduced previously provides several insights in the study of the parameter space of the reinforcement-decay toy model. We thus apply this technique to get insights into the dynamics of purely memristive networks.

In order to study the self-organization properties of memristors, we consider the following mapping between a flow on a network and a stochastic matrix. Given a network with a unique directed edge between two nodes, we introduce the matrix I_{ij} , given by the flow of currents between nodes (i, j) , and defined as a matrix which is elementwise non-negative. For each couple of nodes (i, j) connected by a resistance or memristance, only one of the elements of I_{ij} or I_{ji} are non-zero, depending on the directionality of the current. Since I is a non-negative matrix, we can obtain a stochastic matrix by normalizing by rows (columns), obtaining \tilde{I} , satisfying $\sum_j \tilde{I}_{ij} = 1$ ($\sum_i \tilde{I}_{ij} = 1$). A notion of entropy on the set of currents was introduced in [21] in order to study the self-organizing properties of memristive networks. Here we intend to extend this analysis to understand non-local spatial properties using the graph entropy measure of the previous section.

In order to simulate the dynamical evolution of the memristive network, in the present paper we use nodal analysis [33] to solve for the currents at each time step, and a Runge-Kutta 4 method to implement the dynamics. We then construct the Markov matrix from the resulting currents, and calculate the node entropy dynamically.

A particular feature we aim to explore is the role of symmetry. In Fig. 1 we introduce the triangular network with $L = 3$ layers which can be easily generalized recursively. In each layer, there are both horizontal memristors closing on a triangular mesh, and vertical memristors connecting to a new layer. For a triangular network with L layers, there are $3 * (2^L - 1)$ memristors to simulate. In the last layer, the horizontal memristors are not placed, as these have zero voltage difference applied to them due to the connection to the ground. Let us consider first the case in which there is no state decay, $\alpha = 0$, and in which all the polarities of the memristors are aligned alike $p = 1$. In particular, we simulate homogeneous memristors parameters, with $R_{on} = 100$ Ohm, $R_{off} = 16000$

Ohm, $\mu = 10^{-3}$, $D = 10^{-11}$, and with a time step given by $dt = 10^{-2}$ s = cs and with constant external voltage $V = 50$.

As a first example, we consider the case $L = 4$ under the forcing of an AC generator voltage generator $V(t) = 10 \sin(10t)$, shown in Fig. 3 (upper figure), for a random initialization of the memristor state. We note immediately that the negative and positive voltage sides of the generators correspond to different phases of the circuit. In fact, it is easy to see that the node entropy changes dramatically and periodically with time, following the change of currents signs. The case of a DC generator is shown in Fig. 3 (left panel) for an initial random configuration. Interestingly, from the entropy we can identify the 4 different layers of memristors asymptotically. We note that initially, being each memristor randomly initialized, each node has different entropy level. We note that this non-local entropy measure is sensitive to changes in different nodes of the network, as it can be easily observed. However, we observe that during the dynamics the node belonging to each layer reaches a level of entropy common to all the other nodes. The fourth layer has entropy zero since it is connected to the ground, and only a unique current is connected to the node.

A similar behavior is observed also for tree networks with a higher number of layers, as shown in Fig. 4 for the cases $L = 5, 6$ and 7 . Few peculiar things can be noted. First, we note that the number of layers is equal to the number of asymptotic levels of the entropy, and the number of nodes with that level of entropy corresponds exactly with the number of nodes in that layer (for the L -th layer, there are 2^{L-1} nodes). Moreover, we note that the time it takes for the entropy to reach its asymptotic value increases with the number of layers. Visually, one can observe that it is ≈ 20 s for $L = 4$, 30 s for $L = 5$, ≈ 60 s for $L = 6$ and ≈ 120 s for $L = 7$. This is confirmed in Fig. 6 by calculating the histogram of the asymptotic entropy value for the cases $L = 4, 5, 6, 7$.

We noted performing the simulations that the thermalization time increased with the number of layers; the thermalization time is considered as the time it takes to the entropy to reach its asymptotic value. We observed then, that interestingly if the frequency of the generator in the AC mode is longer than twice the thermalization time, then in the negative voltage part of the generator, the node entropy is zero. This is shown for instance in Fig. 4 for the case of $L = 4, L = 5$ and $L = 6$, and where the frequency has been tuned to be larger than the thermalization time. In the negative side of the generator, the system can be described by, instead of the forward probabilities, by the backward probabilities, implying that the stochastic matrix is derived from the transpose of the current matrix I_{ij} . The difference is shown in Fig. 7, which clarifies that the positive voltage of the generator is characterized by the forward probabilities matrix, but the negative side is characterized by the backward probabilities.

This has important implications. In particular, it shows

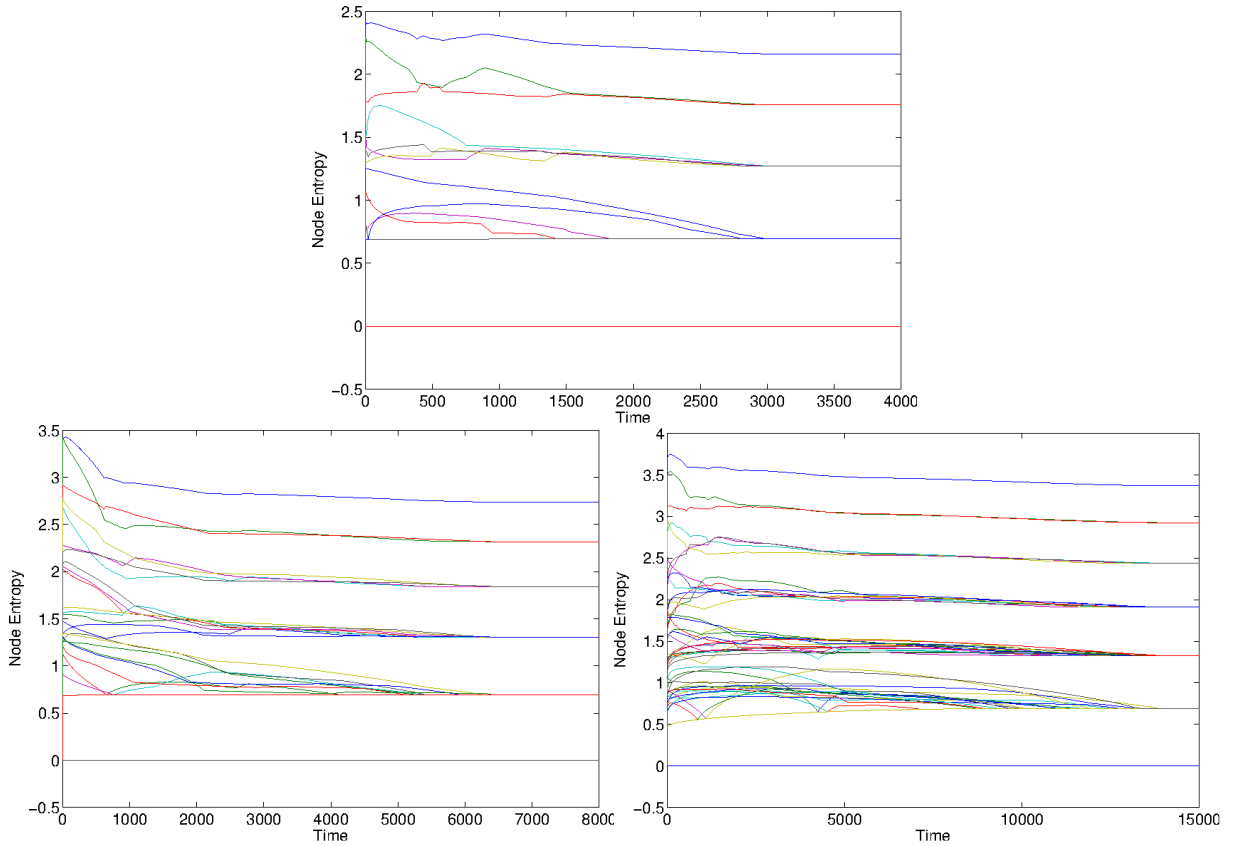


FIG. 4: Graph Entropy for the tree circuit of Fig. 1 for $L=5$ (top), $L=6$ (bottom left) and $L=7$ (bottom right), in the case of DC generator, with $V_0 = 60$ volts. The initial configurations are chosen at random. We observe the emergence of L layers of entropy, showing that the system self-organized in order for the nodes in each layers to have equal entropy.

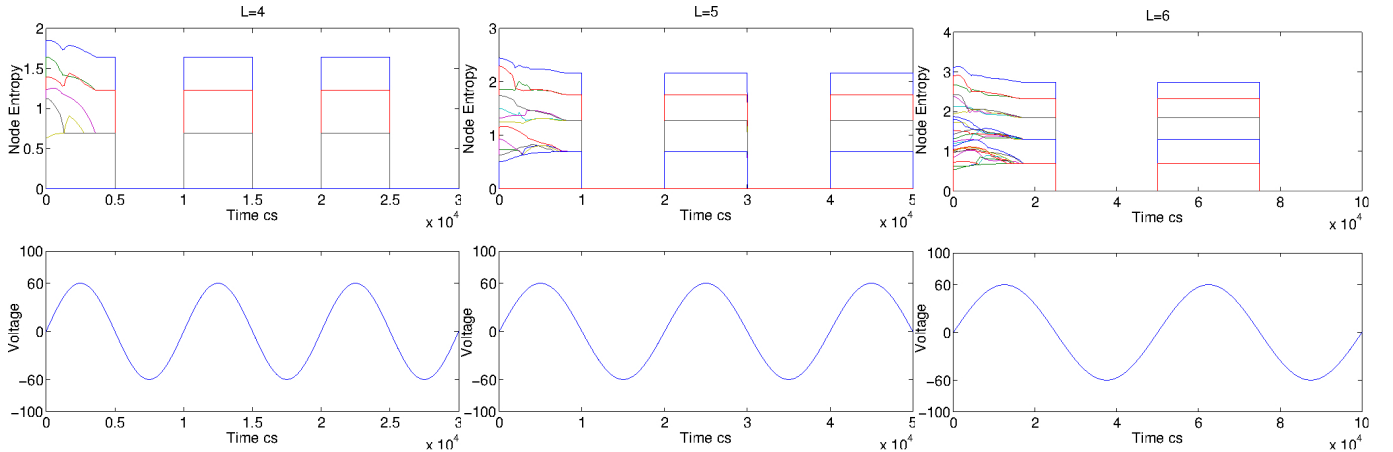


FIG. 5: Node complexity based on forward probability for the case of $L = 4$, $L = 5$ and $L = 6$ networks, for a single instance from random initial configuration of the memristors. The frequency has been tuned to let the system thermalize in the upside of the voltage generator. We see that in the negative part of the voltage generator, the entropy becomes zero.

that asymptotically the memristive network considered here converges to a state which respects the symmetry of the network. The fact it converges to a specific value, although surprising to be unique, can be thought as a feature of the network. However, the more surprising fact is that the node entropy is symmetry respecting. Given

the non-locality of the measure, all the nodes converge altogether to their asymptotic values. Moreover, since it starts from random configuration of the memristors, this implies that the symmetry-respecting state is an attractor of the system. We also observe the network rearranges itself in order to make superfluous some of

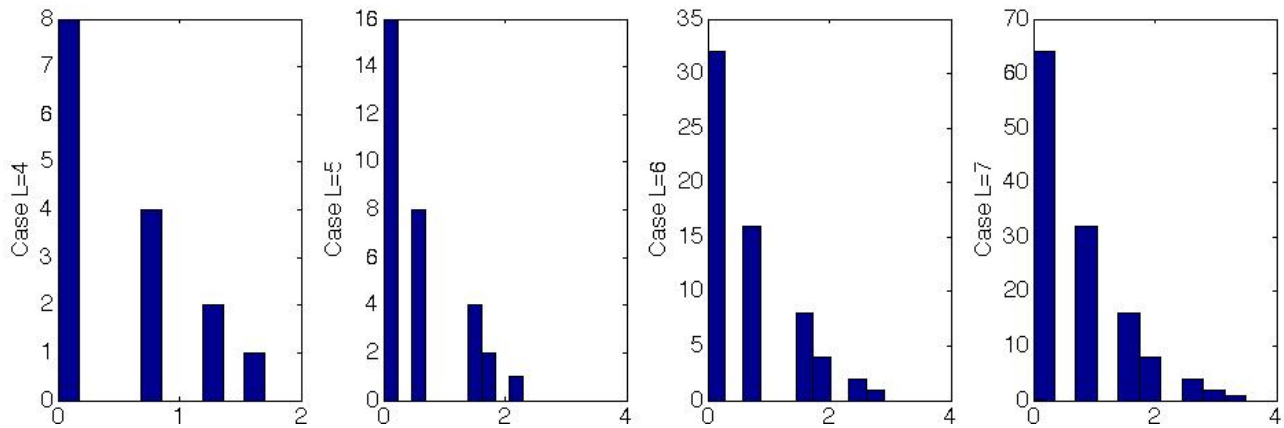


FIG. 6: Histograms of the asymptotic entropy values for $L = 4, 5, 6, 7$. We observe that the maximum entropy increases, and that the number of values on each level scales as 2^L .

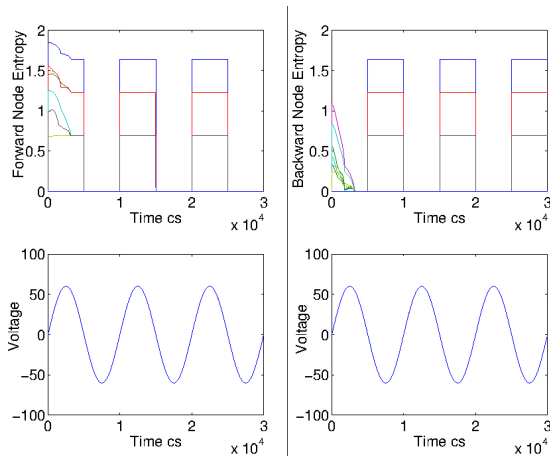


FIG. 7: We show the difference between the node complexity measure based on forward probability and backward probability in the case of AC controlled memristive circuits. If the frequency is lower than the inverse of the half thermalization time, then the entropy is zero in the negative voltage part of the generator, as the left plot shows. In this case, one has to use backward probabilities, as in the right plot.

the memristances. It is easy in fact to realize that since the nodes in a layer must be equal, the memristances arranged horizontally and belonging to the same layer are connected to nodes of equal voltage. This implies that no current is flowing in these memristances.

An extension of the model above can be made to account for both state decay and different polarities. We simulate for simplicity the case $L = 4$ and with the polarity assigned at random with equal probability, and for $\alpha = 0.5$. In Fig. 8 (top left) we show the case already simulated with $p = 1$ and $\alpha = 0$, and the result of a Monte Carlo simulation of 100 initial conditions randomizations. In Fig. 8 (top right) the case with $\alpha = 0.5$ and $p = 1$. In Fig. 8 (bottom left), we simulate otherwise p

assigned at random and $\alpha = 0.5$, and in Fig. 8 (bottom right) the case with both random polarities and state decay. Some notable differences can be observed. In the case with state decay, the memristive network reaches the same asymptotic entropy configuration as the case with no state decay, although dynamically these have very different behavior. In the case with switched polarities, the network symmetry is lost, as now each memristor has different alignment. We see then in this case that both in the case with and without state decay the node entropies reach completely different asymptotic values.

To conclude, we provide the sensitivity analysis of the graph entropy as a function of the applied voltage in the case of the DC voltage, no state decay and aligned polarities in Fig. 9. we plot the asymptotic entropy values for each node in the case $L = 5$ (left), and the derivative with respect to the voltage (right). These have been obtained after a Monte Carlo average over the initial random initialization of the memristor internal parameters, and averaged over 100 instances. We note that there is a critical value of the voltage applied by the generator, called V_c , after which the asymptotic complexity does not change anymore. Although we stress that the actual value of V_c depends on the parameters characterizing the memristors, after variation of the parameters we find a similar behavior. In Fig. 9 (right) we see that the derivative of the entropy becomes zero. Further analysis, beyond the scope of this paper, is required to understand whether this transition presents any form of critical behavior.

IV. DISCUSSION

In this paper we applied the complexity measure introduced in [23] to study the evolving complexity of dynamical graphs, in particular the case of the toy model of [14], inspired by evaporating ant pheromone trails, a process known to be able to solve problems as finding the shortest path between their nest and food by leaving

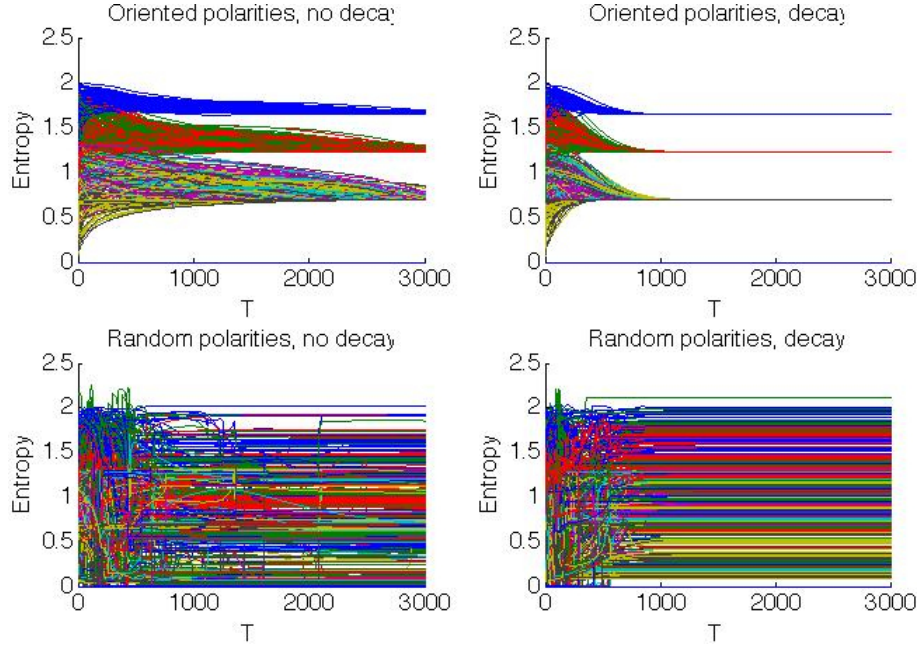


FIG. 8: Comparison between simulations without state decay and aligned polarities (top left), only state decay (top right), randomized polarities (bottom left), and randomized polarities with state decay (bottom right). The plots were obtained from plotting all the results from 100 Monte Carlo simulations with similar dynamical parameters but where the initial states have been randomized.

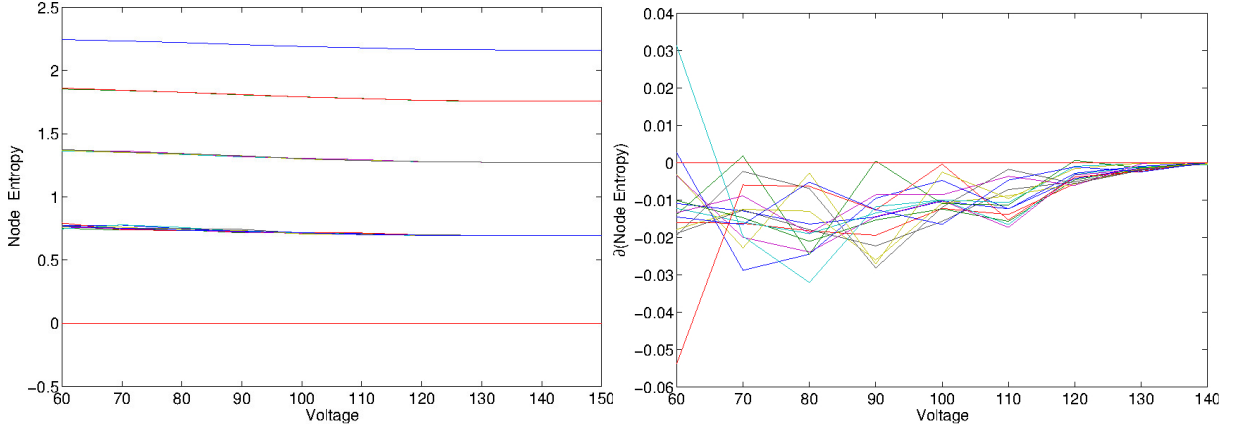


FIG. 9: Average Node entropy (left) evaluated from a Monte Carlo simulations over 100 instances, in the case $L = 5$. The voltage is varied from $V = 60$ to $V = 150$ in steps of 10 volts. On the left, we plot the derivative of the entropy wrt the input voltage. We observe that for large values of the voltage, the derivative converges to zero. Multiple simulations have shown that the value of V where the derivative crosses zero is not universal, but indeed varies with the parameters of the memristors.

a pheromone track that has a characteristic decay time, but which is reinforced every time other ants use it. We have also applied the complexity measure to the case of pure memristive networks [18, 19]. A local version of the entropy used in this paper was in fact introduced in [21] to study the self-organization properties of memristors. This non-local entropy can be thought as the centrality operator applied to the local definition of entropy of a node in a graph, the one used in [21], and depends on an external constant which controls the amount of non-locality. This

allowed the study of the transient behavior of the entropy. We fixed this parameter to encompass all the nodes in the network. This also fixes the maximum entropy one can expect from a node, and have provided a formula for it. The features of this entropy were studied numerically both for the reinforcement-decay model and for the case of memristive networks arranged as a recursive tree with horizontal memristors. We considered these two models and their relaxation to the asymptotic fixed points. Although being not of general character, we have observed

that the non-local complexity measure introduced here characterizes the asymptotic graph structure. For the case of the reinforcement-decay case, this implies that if for each instance in parameter space, the node entropy takes different values.

The same analysis has been performed for the case of memristive networks, and applied to the case of tree-like structures which can be defined recursively, and shown in Fig. 4. We distinguish here the case of AC and DC controlled circuits. In the case of AC circuits, we have noted that there are two regimes: the one in which the frequency is higher than the inverse of half the thermalization time, and the one in which the frequency is lower. In fact, in general the entropy reveals that the memristive network self-organizes, reaching a configuration in which each node in the k -th layer has the same entropy. If the frequency in the AC controlled circuit is low enough that the memristors thermalize, in the negative voltage side of the sinusoid the entropy of the network becomes zero. We have shown that in this case, one has to consider both the forward and backward probabilities to characterize the network. We moreover considered the case in which the polarities of the memristors were chosen at random, and the dynamics of the internal parameter has been extended to consider state decay. In the former case the symmetry of the graph is destroyed, and thus one observes that the asymptotic entropy configuration can take any value depending on the initial conditions. In the latter case, the state decays does not change the entropy configuration, although the convergence is faster. As a last comment, we have shown that in general the asymptotic level of the entropy for each node depends, in the DC case, on the voltage applied. We have shown, however, that if the voltage is high enough, the entropy converges to a fixed value. This value changes depending on the parameter of the model, and thus is not universal. The analysis of this phenomenon goes beyond the scope of this paper, and will be analyzed in future works, but shows that the entropy considered in this paper has interesting properties.

The finding of this article then suggest that non-local measures of self-organization are not only useful at *compressing* information about the properties of graphs which are changing dynamically, but that these can provide several insights about the dynamics itself. We have also noted that when applying these methods to the case of directed graphs, then these measures can give not insightful indications if for instance flows change suddenly signs. We should stress that these findings cannot be made general (i.e. to graphs and model other than the one studied), and they turn out being only descriptive, rather than *predictive*. However, we believe that the graph entropy studied here does provide a compact way of compressing most of the degrees of freedom, and shifting these from the edges of the graph, to the nodes. For graphs in which the number of edges is much larger than the number of nodes, this might allow for instance the use of *heat maps* to classify and study the type of dynamics. The work done in this paper shows this feature clearly. As a closing remark, we believe that this entropy has better asymptotic properties (long walks) as compared to those introduced in [21], and thus can be used to study the thermalization properties of memristive networks.

In much more general terms, our study provides a connection between self-organization, non-locality and entropy-based measures. We thus hope our work will motivate further theoretical and experimental studies along these directions.

Acknowledgments

F.C. would like to thank Alioscia Hamma, Massimiliano Di Ventra and Fabio Traversa for discussion on the results of this work, and the anonymous referee for raising few interesting points which improved the quality of the paper. *Funding* F.C. acknowledges support from Invenia Labs.

-
- [1] R. Albert and A. L. Barabasi, *Reviews of Modern Physics* **74** **47** (2002).
 - [2] D. J. Watts and S. H. Strogatz, *Nature* **393**, 440 (1998).
 - [3] G. Caldarelli, *Scale-Free Networks* (Oxford University Press, Oxford, 2007).
 - [4] A. Barrat, M. Barthélemy, and A. Vespignani, *Dynamical Processes on Complex Networks* (Cambridge University Press, Cambridge, UK, 2009).
 - [5] M. E. J. Newman, *Networks: An Introduction* (Oxford University Press, Oxford, 2010).
 - [6] E. Estrada, *The Structure of Complex Networks: Theory and Applications* (Oxford University Press, Oxford, 2011).
 - [7] S. N. Dorogovtsev, A. V. Goltsev, and J. F. F. Mendes, *Phys Rev. E* **65**, 066122 (2002).
 - [8] T. S. Evans and J. P. Saramaeki, *Phys Rev. E* **72**, 026138 (2005).
 - [9] J. P. Saramaeki and K. Kaski, *Physica A* **341** (2004).
 - [10] J. M. Kleinberg, in *Proceedings of the ACM-SIAM Symposium on Discrete Algorithms* (1998).
 - [11] M. Li, L. Gao, Y. Fan, J. Wu, and Z. Di, *New J. Phys* **12**, 043029 (2010).
 - [12] O. Chrysafis and C. Cannings, *Physica A* **388** (2009).
 - [13] N. Ikeda, *J. Math Theor Phys* **41**, 05 (2008).
 - [14] F. Caravelli, A. Hamma, and M. Di Ventra, *EPL* **109** ((2015)).
 - [15] M. Di Ventra and Y. V. Pershin, *Nanotechnology* **24** (2013).
 - [16] J. Buhl and et al., *Eur Phys. J. B* **42** (2004).
 - [17] F. Schweitzer, K. Lao, and F. Family, *Biosystems*. **41**, 153 (1997).
 - [18] D. B. Strukov, G. Snider, D. R. Stewart, and R. S. Williams, *Nature* **453** (2008).
 - [19] L. O. Chua, *IEEE Transactions on Circuits Theory* **18**, 507 (1971).

- [20] Y. Pershin and M. Di Ventra, Phys Rev. E **84**, 046703 (2011).
- [21] Y. Pershin and M. Di Ventra, Phys Rev. E **88**, 013305 (2013).
- [22] F. L. Traversa, C. Ramella, F. Bonani, and M. Di Ventra, Science Advances **1** (2015).
- [23] F. Caravelli, Chaos, Solitons and Fractals **73**, 90 (2014).
- [24] S. Lloyd and H. Pagels, Ann. of Phys. **188** (1988).
- [25] K. Lindgren, Phys. Rev. A **38**, 9 (1988).
- [26] L. Ekroot and T. M. Cover, IEEE Transactions on Information Theory **39**, 4 (1993).
- [27] P. Kloeden and E. Platen, *Numerical Solution of Stochastic Differential Equations*, vol. 23 (Springer, 1999).
- [28] M. Di Ventra and Y. V. Pershin, Nature Physics **9**, 200 (2013).
- [29] M. Di Ventra, Y. Pershin, and L. Chua, Proceedings of the IEEE **97** **97** (2009).
- [30] T. Ohno, T. Hasegawa, A. Nayak, T. T. and J.K. Gimzewski, and M. Aono, Applied Physics Letters **20** (2011).
- [31] A. V. Avizienis, H. O. Sillin, C. Martin-Olmos, H. H. Shieh, M. Aono, A. Z. Stieg, and J. K. Gimzewski, Plos ONE **8** (2012).
- [32] J. P. Carbajal, J. Dambre, M. Hermans, and B. Schrauwen, Neural Computation **27**, 725 (2015).
- [33] P. Horowitz and W. Hill, *The Art of Electronics (Second ed.)*, (Cambridge University Press, Cambridge, UK, (1989)).